

## Measurement of thermal properties of soil and concrete samples

Pagola, Maria Alberdi; Jensen, Rasmus Lund; Madsen, Søren; Poulsen, Søren Erbs

*Publication date:*  
2017

*Document Version*  
Publisher's PDF, also known as Version of record

[Link to publication from Aalborg University](#)

*Citation for published version (APA):*

Pagola, M. A., Jensen, R. L., Madsen, S., & Poulsen, S. E. (2017). *Measurement of thermal properties of soil and concrete samples*. Aalborg University. Department of Civil Engineering. DCE Technical Reports No. 235

### General rights

Copyright and moral rights for the publications made accessible in the public portal are retained by the authors and/or other copyright owners and it is a condition of accessing publications that users recognise and abide by the legal requirements associated with these rights.

- Users may download and print one copy of any publication from the public portal for the purpose of private study or research.
- You may not further distribute the material or use it for any profit-making activity or commercial gain
- You may freely distribute the URL identifying the publication in the public portal -

### Take down policy

If you believe that this document breaches copyright please contact us at [vbn@aub.aau.dk](mailto:vbn@aub.aau.dk) providing details, and we will remove access to the work immediately and investigate your claim.



**DEPARTMENT OF CIVIL ENGINEERING**  
AALBORG UNIVERSITY

# **Measurement of thermal properties of soil and concrete samples**

**Maria Alberdi-Pagola**

**Rasmus Lund Jensen**

**Søren Madsen**

**Søren Erbs Poulsen (VIA University College, Horsens, DK)**



Aalborg University  
Department of Civil Engineering

**DCE Technical Report No. 235**

# **Thermal property measurements of soil and concrete samples**

by

Maria Alberdi-Pagola  
Rasmus Lund Jensen  
Søren Madsen  
Søren Erbs Poulsen (VIA University College)

December 2017

© Aalborg University

## Scientific Publications at the Department of Civil Engineering

**Technical Reports** are published for timely dissemination of research results and scientific work carried out at the Department of Civil Engineering (DCE) at Aalborg University. This medium allows publication of more detailed explanations and results than typically allowed in scientific journals.

**Technical Memoranda** are produced to enable the preliminary dissemination of scientific work by the personnel of the DCE where such release is deemed to be appropriate. Documents of this kind may be incomplete or temporary versions of papers—or part of continuing work. This should be kept in mind when references are given to publications of this kind.

**Contract Reports** are produced to report scientific work carried out under contract. Publications of this kind contain confidential matter and are reserved for the sponsors and the DCE. Therefore, Contract Reports are generally not available for public circulation.

**Lecture Notes** contain material produced by the lecturers at the DCE for educational purposes. This may be scientific notes, lecture books, example problems or manuals for laboratory work, or computer programs developed at the DCE.

**Theses** are monographs or collections of papers published to report the scientific work carried out at the DCE to obtain a degree as either PhD or Doctor of Technology. The thesis is publicly available after the defence of the degree.

**Latest News** is published to enable rapid communication of information about scientific work carried out at the DCE. This includes the status of research projects, developments in the laboratories, information about collaborative work and recent research results.

Published 2017 by  
Aalborg University  
Department of Civil Engineering  
Thomas Manns Vej 23  
DK-9000, Aalborg Ø, Denmark

Printed in Aalborg at Aalborg University

ISSN 1901-726X  
DCE Technical Report No. 235

## Table of contents

List of figures .....	5
List of tables.....	6
List of acronyms.....	6
1. Introduction.....	7
2. Methods.....	7
2.1. Thermal properties.....	7
2.2. Other physical properties affecting thermal properties .....	8
2.3. Prediction models of thermal properties of concrete .....	8
3. Thermal properties of soil.....	10
3.1. Langmarksvej .....	10
3.1.1. Soil description .....	11
3.1.2. Measurements .....	12
3.2. Rosborg Gymnasium .....	13
3.2.1. Soil description .....	14
3.2.2. Measurements .....	15
4. Thermal properties of concrete .....	16
4.1. Experimental characterisation.....	16
4.1.1. Mix constituents and test specimens.....	16
4.1.2. Measurements .....	16
4.2. Application of prediction models of thermal properties .....	20
4.3. Discussion .....	20
5. Conclusion.....	21
6. Acknowledgements.....	22
7. References .....	22
8. Appendices.....	24
A) Soils.....	24
B) Concrete.....	26
Measurement process and parameters.....	26
Oven drying and saturating concrete specimens.....	27
Measuring relative humidity in GeoLab and determining water content of normally dried specimens .....	27
Mineralogical analysis.....	28
Thermal property values from literature.....	29

## List of figures

Figure 1: a) Hot Disk apparatus set up at the GeoLab at VIA University College, Horsens, DK; b) Sample holder for small samples, such as the shown steel standard cylinders. ....	8
Figure 2: The Langmarksvej test site, Langmarksvej 84, 8700 Horsens, Denmark. ....	10
Figure 3: Soil description of the samples collected each 0.5 m in the drilling executed at Langmarksvej. Legend according to DGF Bulletin 1 (Larsen, G., 1995). ....	11
Figure 4: Stratigraphic profile at the Langmarksvej test site. Bulk density $\rho$ , water content, thermal conductivity $\lambda_s$ and volumetric heat capacity $\rho c_p$ measured in the laboratory using the Hot Disk apparatus are also provided. $\rho c_{p \text{ eff}}$ and $\lambda_{s \text{ eff}}$ are weighted average estimates over the length of the drilling. ....	12
Figure 5: The Rosborg Gymnasium building at Vestre Engvej 61, 7100 Vejle, Denmark. The south and north extensions are founded on 200 and 220 energy piles, respectively. ....	13

Figure 6: Soil description of the samples collected each 0.5 m in the drilling executed at Rosborg North.....	14
Figure 7: Stratigraphic profile at Rosborg Norht test site. Bulk density $\rho$ , water content, thermal conductivity $\lambda_s$ and volumetric heat capacity $\rho c_p$ measured in the laboratory using the Hot Disk apparatus are also provided. $\rho c_{p \text{ eff}}$ and $\lambda_{s \text{ eff}}$ are weighted average estimates over the length of the drilling. ....	15
Figure 8: Measured thermal properties of S3 receipt concrete with the transient plane source method. The error bars indicate the 95% confidence level. ....	18
Figure 9: Average of measured thermal properties of S3 receipt concrete with the transient plane source method. The error bars indicate the 95% confidence level. Average values for 4 specimens, according to ASTM C642-13: volume of permeable voids: $8.6 \pm 0.8\%$ ; absorption = $3.7 \pm 0.3\%$ ...	19
Figure 10: Predicted thermal properties of concrete against experimentally obtained values a) volumetric heat capacity $\rho c_p$ and b) thermal conductivity $\lambda$ . ....	21
Figure 11: a) Halved moraine clay sample. b) Hot Disk kapton sensor ready to be placed between two specimens of soil. c) On-going Hot Disk testing, two-side measurement of a moraine clay sample (depth 8.5 m at Langmarskvej test site). ....	24
Figure 12: a) Hot Disk kapton sensor (15 mm in diameter) ready to be placed between two specimens of a silty sand sample. b) On-going Hot Disk testing, two-side measurement of the silty sand sample (depth 1.0 m at Rosborg North site). ....	24
Figure 13: a) Sand sample in a container; b) On-going Hot Disk test, single-sided measurement of a sand sample (depth 4.5 m). ....	25
Figure 14: a) Hot Disk kapton sensor (15 mm in diameter) ready to be placed between two specimens of concrete. b) On-going Hot Disk testing, two-side measurement of a concrete sample. ....	26
Figure 15: Weight evolution over oven-drying process for each specimen. Concrete drying at 105 °C. ....	27
Figure 16: Desiccator. ....	27
Figure 17: temperature and relative humidity measurements in the GeoLab at VIA University College in Horsens (DK). ....	28

## List of tables

Table 1: Mix components and physical properties for the S3 receipt. Average values for the two batches. The dosage is kept confidential. ....	16
Table 2: Measured porosity and absorption of the concrete specimens. ....	17
Table 3: Summary of samples and measurements for each condition.....	17
Table 4: Summary of mean values of the thermal property property measurements and their uncertainties. ....	18
Table 5: Thermal properties of the concrete components assumed for the prediction models.....	20
Table 6: Summary of recommended experimental parameters for different soils based on measurements performed at the GeoLab at VIA University College, Horsens, DK, for the present study. ....	25
Table 7: Summary of recommended experimental parameters for concrete specimens based on measurements performed at the GeoLab at VIA University College, Horsens, DK, for the present study. ....	26
Table 8: Mineralogical analysis of sand 0-2 mm.....	28
Table 9: Mineralogical analysis of sand 4-8 mm.....	28
Table 10: Thermal property values considered for prediction models.....	29

## List of acronyms

RN: Rosborg Gymnasium North extension  
LM: Langmarksvej test site

# 1. Introduction

Centrum Pæle A/S, Aalborg University, VIA University College and INSERO Horsens are partners in an industrial PhD project within the field of shallow geothermal energy systems based on pile heat exchangers. Pile heat exchangers, also known as energy piles, are thermally active building foundation elements with embedded geothermal pipes fixed to the steel reinforcement in which a circulating fluid exchanges heat with the pile and the surrounding soil. As such, the foundation of the building both serves as a structural component and a heating/cooling supply element. The thermal properties of the pile-soil system, therefore, influence the operational performance of the ground source heat pump system.

This document aims to present the laboratory work undertaken to analyse the thermal properties of the soil at two test sites in Denmark and the concrete produced by Centrum Pæle A/S, used to produce the pile heat exchangers studied in the present PhD project. The tasks have been carried out between February 2016 and February 2017.

The presented work mainly consists of thermal property measurements. They become important as they form the basis for dimensioning a planned ground source heat pump installation based on closed loop vertical ground heat exchangers. This report complements the report “Thermal response testing of precast pile heat exchangers: fieldwork report” by (Alberdi-Pagola et al., 2017).

The report is organized as follows: first, the measurement methods and the test procedures are described. Second, the soils at both test sites are described, together with the measurements. Third, the measurements of the properties of the concrete are treated. The work is extended in appendixes.

## 2. Methods

Both soil and concrete samples are treated in a similar way. Each sample is properly described and its thermal properties, water content and bulk and dry densities are measured. The thermal expansion is not measured in this study. The thermal properties experimentally determined for the concrete are compared with the estimates from selected prediction models. To double-check the reliability of the measurements, the measurements are compared to literature values.

### 2.1. Thermal properties

The thermal properties have been measured by means of a Hot Disk apparatus (Figure 1). The Hot Disk equipment relies on the transient plane source method (Hot Disk AB, 2014) according to the Dansk Standard (2015) DS/EN ISO 22007-2 (2015). The transient plane source method yields estimations on the thermal conductivity  $\lambda$  [W/m/K], volumetric heat capacity  $\rho c_p$  [MJ/m<sup>3</sup>/K]. Thermal diffusivity  $\alpha$  [m<sup>2</sup>/s] is defined as the ratio between the thermal conductivity and volumetric heat capacity.

The Hot Disk sensor is an electrically conducting metallic double spiral (nickel), covered by two thin layers of insulating material (kapton). During the measurement, the sensor is placed between two pieces of sample. As the electrical current runs, the temperature of the sensor increases and at the same time, the temperature resistance as a function of time is measured. Hence, the sensor acts as a heat source and a dynamic temperature sensor. Hot Disk AB (2014) defines the accuracy of the thermal conductivity measurements as  $\pm 5\%$ , while the accuracy for the thermal diffusivity is defined between  $\pm 5$  and  $10\%$ . The uncertainty for the average value of the measurement  $\bar{x}$  is defined as their root-sum-squared relation of the systematic and random errors for 95% confidence level:

$$w_{\bar{x}} = (B_{\bar{x}}^2 + P_{\bar{x}}^2)^{1/2} \quad (1)$$



Five repeated measurements have been taken for each sample at a room temperature between 19 to 21 °C.

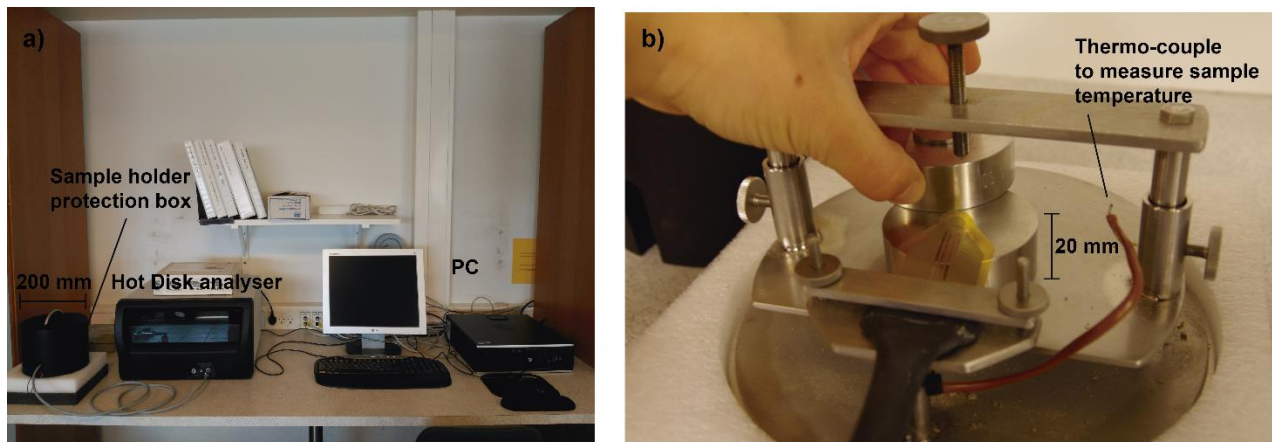


**Figure 1: a) Hot Disk apparatus set up at the GeoLab at VIA University College, Horsens, DK; b) Sample holder for small samples, such as the shown steel standard cylinders.**

## **2.2. Other physical properties affecting thermal properties**

The soil specimens are characterised under “undisturbed” conditions. The water content has been measured following the DS/EN ISO/TS 17892-1: 2004 (2004) standard and the bulk and dry density determination follow the DS/EN ISO/TS 17892-2: 2004 (2004). The organic matter content has been measured following the ASTM Standards (1998).

Regarding the concrete, the determination of potential lower and upper bounds of its thermal properties are aimed. Under operational conditions, the pile heat exchanger will be driven into a medium that could have different moist content. This means that the saturation process is governed by the capillary domain. Therefore, the maximum water content that the material can acquire by suction, water pressure or condensation will be higher than the one absorbed by being in contact with air and it could reach 10 % in weight, depending on the concrete. Therefore, a range of thermal properties is targeted and the samples are measured in oven dry, saturated and normally dry (ambient air) conditions. The drying and the saturation processes and the density, absorption and voids in hardened concrete measurements are determined following the ASTM Standards (2013). The samples were allowed to “normally dry”, from the saturated condition, under normal ambient surroundings for times extended over 6-7 days. The samples were oven dried again to determine the water content of the last measurement. The test are performed in samples with a curing time of more than a month.

## **2.3. Prediction models of thermal properties of concrete**

As a further step, prediction models reported in the literature to determine the thermal properties of different materials are studied. Concrete is compounded of constituents with a wide variation in thermal properties. The thermal properties of the concrete are affected by: porosity (air and water content), humidity, mineral composition (aggregates and water/cement ratio), particle contact and temperature.

The specific heat of concrete is highly influenced by moisture content, aggregate type, cement type and density of concrete (Khaliq and Kodur, 2011). For composite materials, such as concrete, it can be calculated by the mixing theory (Bentz et al., 2011):

$$c_{p, \text{ concrete}} = \sum_{i=1}^n c_{p,i} \cdot m_i \quad (2)$$

where  $c_{p,i}$  is the heat capacity of each constituent (cement, water, fly ash, fine and coarse aggregates, etc.) and  $m_i$  refers to the mass fraction of each of those components. However, it has been demonstrated that this model is not applicable to concrete mixtures that contain phase change materials (Pomianowski et al., 2014).

The thermal conductivity is more complex to determine as it is influenced by the way the particles are arranged. Its maximum and minimum values for a two phase system (solid and fluid) with porosity  $\varepsilon$ , are provided by the series and parallel phase distributions, respectively, i.e., by the harmonic and the arithmetic means. As a third option, the geometric mean model assumes a random distribution of phases (Tavman, 1996, Khan, 2002).

For materials where the porosity is large, e.g., powders, granular materials and composites materials (randomly distributed and non-interacting particles in a homogeneous medium), Maxwell's model gives good results (Tavman, 1996).

To consider the influence of admixtures such as silica fume and fly ash on the cement paste, Demirboğa et al. (2007) provide some empirical correlations. Garboczi and Bentz (1992) provided advanced computer simulation models.

Several authors have suggested various thermal conductivity prediction models for traditional concrete mixes (Marshall, 1972, Khan, 2002). The first option was proposed by Campbell and Thorne, described in Marshall (1972) and Khan (2002):

$$\lambda_{\text{concrete}} = \lambda_m \cdot (2M - M^2) + \frac{\lambda_m \cdot \lambda_a \cdot (1 - M)^2}{\lambda_a \cdot M + \lambda_m \cdot (1 - M)} \quad (3)$$

$$M = 1 - \sqrt{1 - p}$$

where,  $p$  is the volume of mortar per unit volume of concrete,  $\lambda$  the thermal conductivity and suffixes "m" and "a" refer to mortar and aggregate, respectively.

The second option is the composite model for conduction or the Hashin-Strikman model, used in Chan (2014), Wadsö L. (2012) and Mehta and Monteiro (2006):

$$\lambda_{\text{concrete}} = \lambda_c + \frac{v_d}{\frac{1}{\lambda_d - \lambda_c} + \frac{v_c}{3 \cdot \lambda_c}} \quad (4)$$

where,  $\lambda_c$  and  $\lambda_d$  are the thermal conductivities of the continuous and particle phases, respectively, and where  $v_c$  and  $v_d$  are the volume of the continuous and particle phases, respectively.

Kim et al. (2003) proposed an empirical relation that yields the thermal conductivity of concrete based on the relationship as functions of aggregate volume fraction AG, fine aggregate fraction S/A, water-cement ratio W/C, temperature T and moisture condition  $R_h$  in concrete. However, this expression requires a referenced thermal conductivity measured from specimens whose receipt is known:

$$\lambda_{\text{concrete}} = \lambda_{\text{ref}} \cdot [0.293 + 1.01 \cdot AG] \cdot \left[ 0.8 \cdot \left( 1.62 - 154 \cdot \left( \frac{W}{C} \right) \right) + 0.2 \cdot R_h \right] \cdot [1.05 - 0.0025 \cdot T] \cdot [0.86 + 0.0036 \cdot \left( \frac{S}{A} \right)] \quad (5)$$

In cases where the nature of the pores within the concrete is known, Khan (2002) compared the Campbell and Thorne model's estimations (Equation 3) to the ones obtained from models developed for porous materials, highlighting the importance of considering the porous state, specially, for mixtures where aggregate conductivity is high.

### 3. Thermal properties of soil

The soil samples are collected in two test sites in Denmark: one in Horsens and another in Vejle.

#### 3.1. Langmarksvej

The test site is situated at Langmarksvej 84 (street address), 8700 Horsens, Denmark (55° 51' 43" N, 9° 51' 7" E), 800 m from the VIA University College campus (Figure 2). The test site was established in 2010 as part of a research collaboration between Centrum Pæle A/S, Horsens A.M.B.A. district heating company and VIA University College. After 4 years without operation, the test site is currently used in the present PhD project.

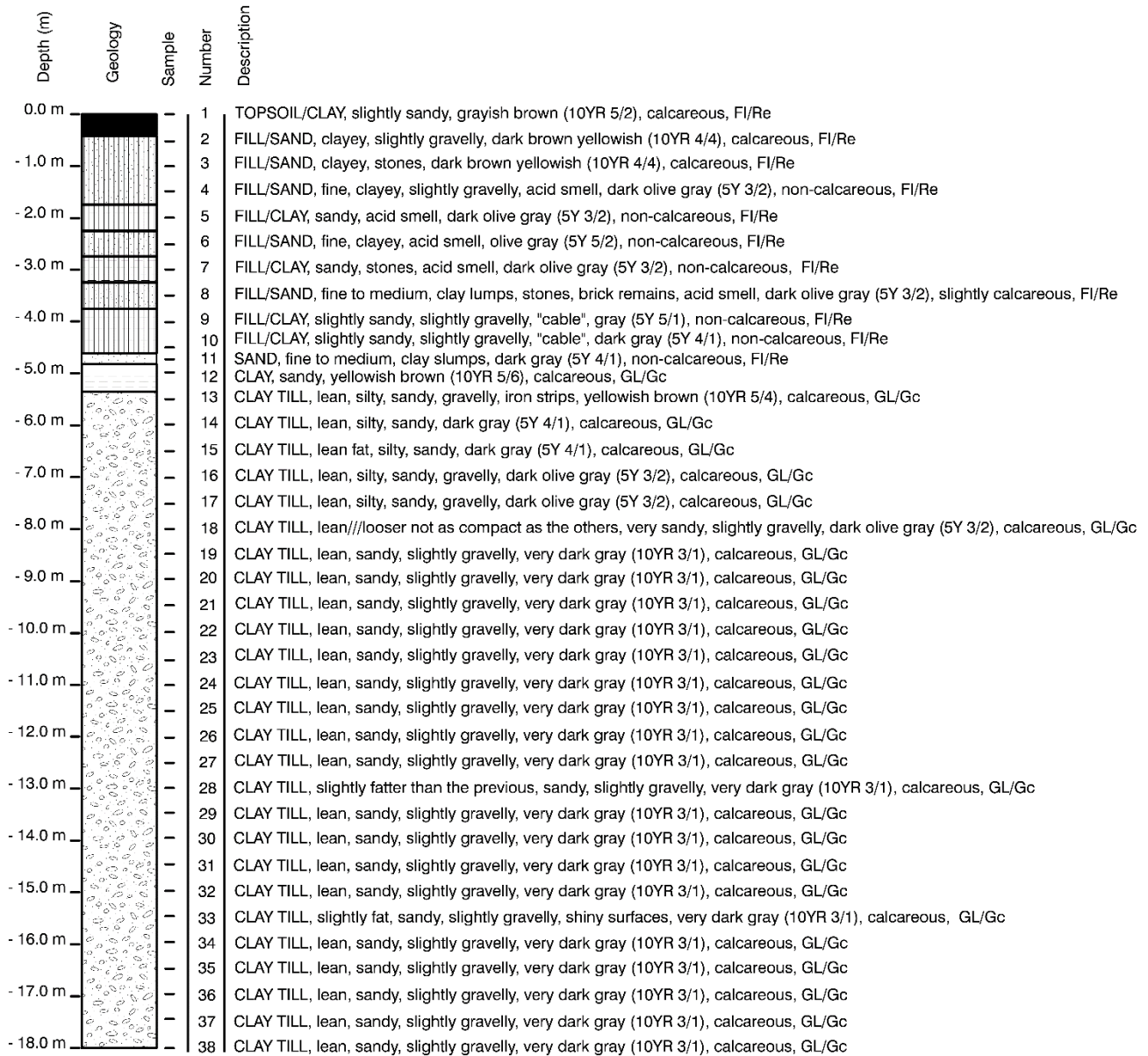
A monitoring drilling was executed 0.85 m apart from one of the pile heat exchangers on the 2/11/2015 by Franck Geoteknik A/S, using the auger drilling technique. Soil samples were collected each 0.5 m and they were kept in sealed plastic bags.



Figure 2: The Langmarksvej test site, Langmarksvej 84, 8700 Horsens, Denmark.

### 3.1.1. Soil description

A stratigraphic column was developed (Figure 3). As depicted, 5 m of fillings emerge on top of glacial clay till.



**Figure 3: Soil description of the samples collected each 0.5 m in the drilling executed at Langmarksvej. Legend according to DGF Bulletin 1 (Larsen, G., 1995).**

### 3.1.2. Measurements

The samples were kept as intact as possible in sealed plastic bags and they were measured within the next 24 - 48 hours. Despite sample number 11 in Figure 3 (sand) which needed to be reconstituted to a realistic density to perform a single sided measurement (see Appendix A), the other samples were cohesive soils and a double side measurement of intact samples could be performed.

Figure 4 illustrates the depth dependence of the bulk density  $\rho$  [g/cm<sup>3</sup>], water content [%], thermal conductivity  $\lambda_s$  [W/m/K] and volumetric heat capacity  $\rho c_p$  [MJ/m<sup>3</sup>/K] of the samples. The weighted average estimates over the length of the drilling give an effective thermal conductivity  $\lambda_s$  of  $2.30 \pm 0.13$  W/m/K and an effective volumetric heat capacity  $\rho c_p$  of  $2.61 \pm 0.27$  MJ/m<sup>3</sup>/K.

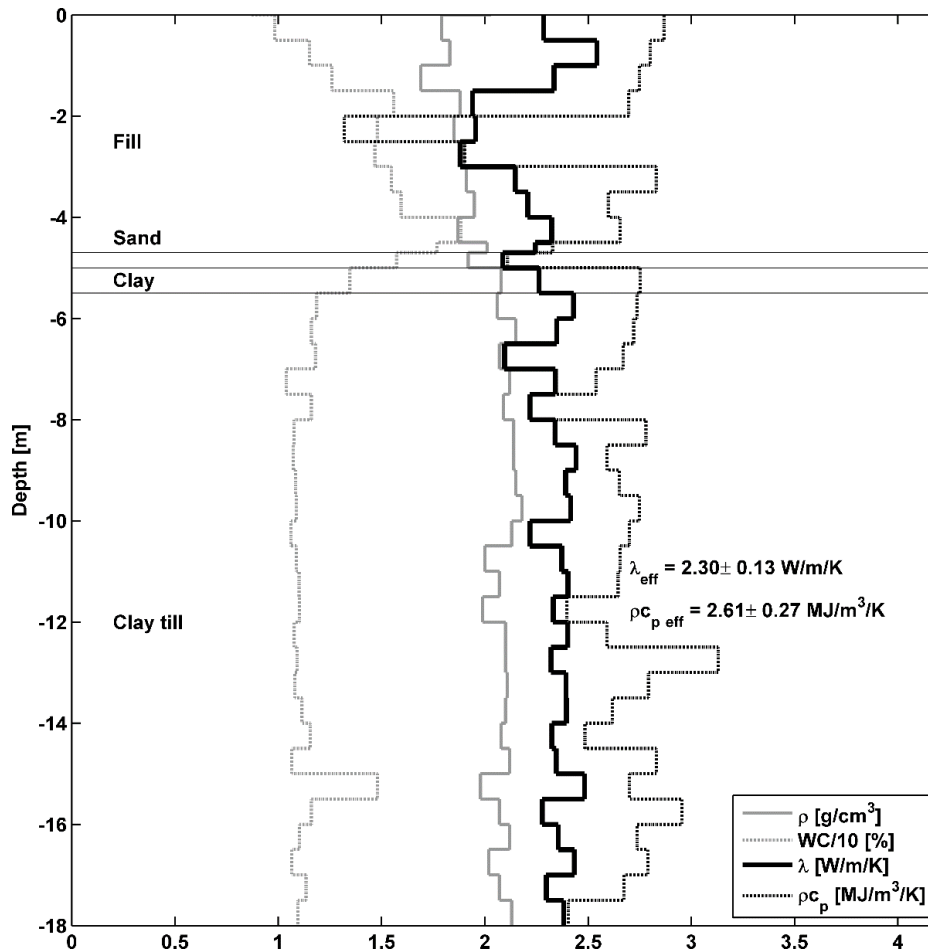


Figure 4: Stratigraphic profile at the Langmarksvej test site. Bulk density  $\rho$ , water content, thermal conductivity  $\lambda_s$  and volumetric heat capacity  $\rho c_p$  measured in the laboratory using the Hot Disk apparatus are also provided.  $\rho c_{p\ eff}$  and  $\lambda_{s\ eff}$  are weighted average estimates over the length of the drilling.



### 3.2. Rosborg Gymnasium

The test site is located at Vestre Engvej 61, 7100 Vejle, Denmark (55° 42' 30" N, 9° 32' 0" E) (Figure 5). The south extension of the Rosborg Gymnasium building is founded on 200 foundation pile heat exchangers. The thermo-active foundation has supplemented the heating and free cooling requirements of the building since 2011 (4,000 m<sup>2</sup> heated area). More information about the performance of the installation can be found in Alberdi-Pagola et al. (2016). The north extension of the gymnasium complex is currently under construction. To date, the foundation, that consists of 220 energy piles, has been constructed. The monitoring drilling was bored 30 meters away from the building towards the north.

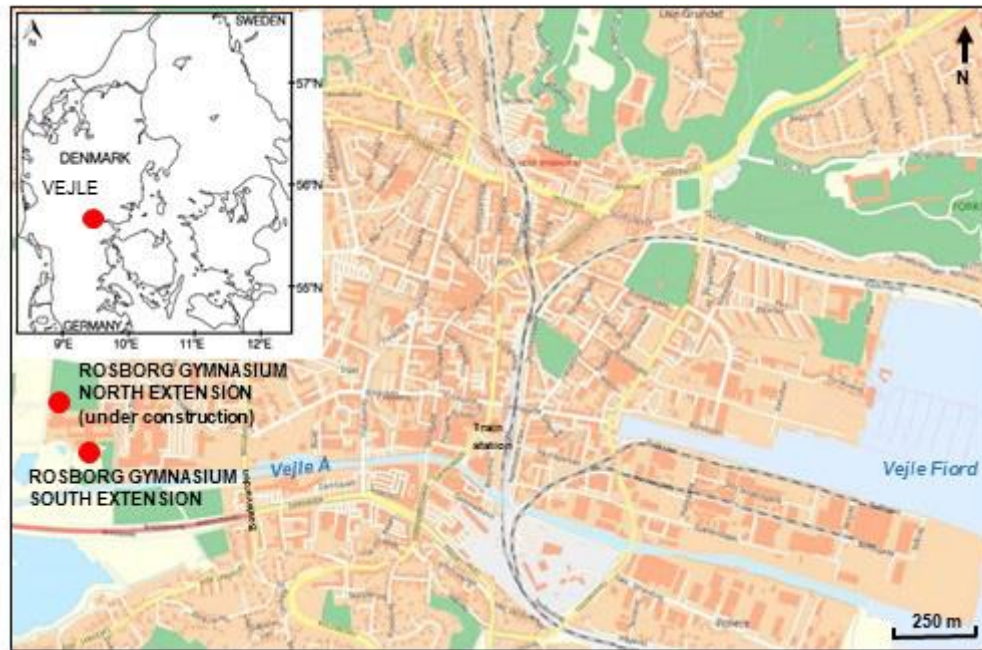
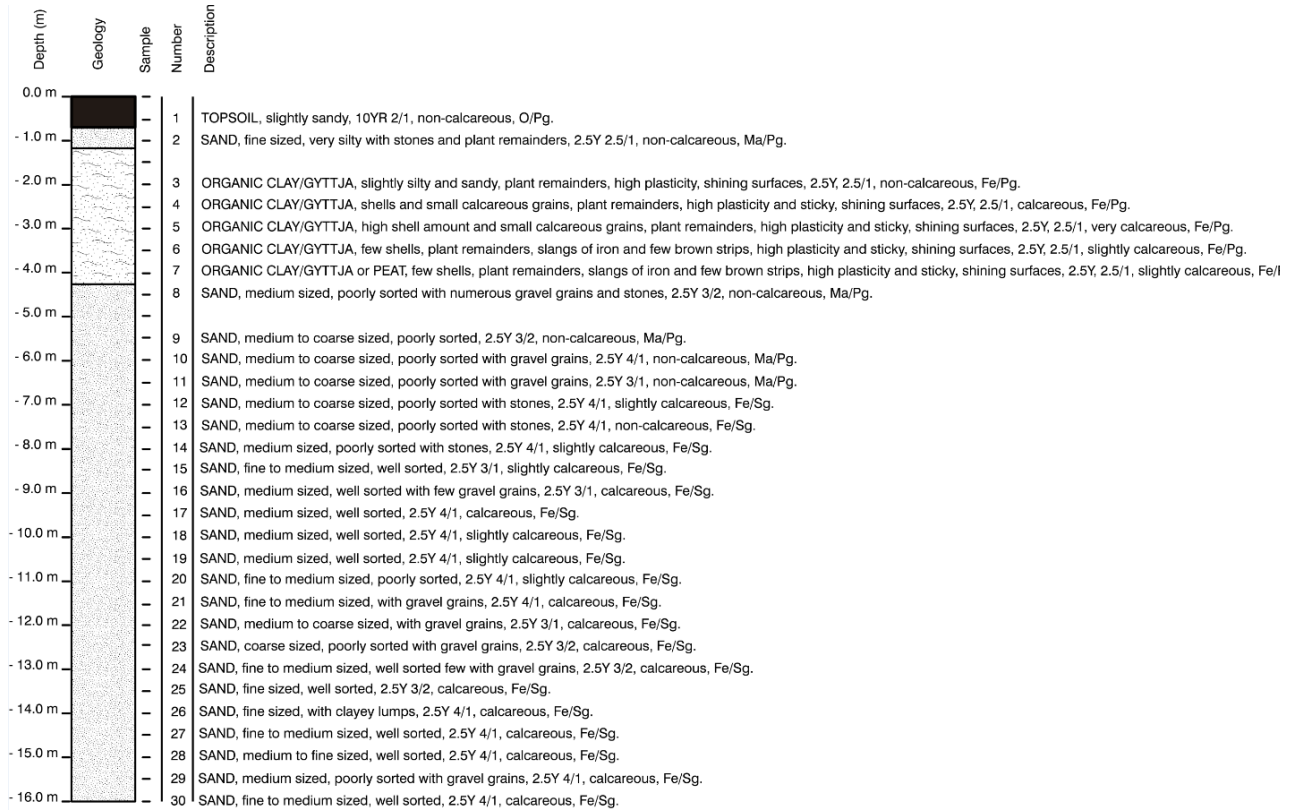


Figure 5: The Rosborg Gymnasium building at Vestre Engvej 61, 7100 Vejle, Denmark. The south and north extensions are founded on 200 and 220 energy piles, respectively.

### 3.2.1. Soil description

A stratigraphic column was developed (Figure 6). The piles are founded in glacial sand 5-6 m below terrain, which is overlain by postglacial, organic mud. The groundwater table is situated around 0.70 m below terrain (Dansk Geoteknik A/S, 1973, Franck Geoteknik A/S, 2013).



**Figure 6: Soil description of the samples collected each 0.5 m in the drilling executed at Rosborg North.**

### 3.2.2. Measurements

The samples were kept as intact as possible in sealed plastic bags and they were measured within the next 24 - 48 hours. Despite samples 1 to 7, which are cohesive, the rest (sand) needed to be reconstituted (repacked and compacted) to a realistic density to perform single sided measurements (see Appendix A).

Figure 7 illustrates the depth dependence of the bulk density  $\rho$  [g/cm<sup>3</sup>], water content [%], thermal conductivity  $\lambda_s$  [W/m/K] and volumetric heat capacity  $\rho c_p$  [MJ/m<sup>3</sup>/K] of the samples. The weighted average estimates over the length of the drilling give an effective thermal conductivity  $\lambda_s$  of  $2.14 \pm 0.11$  W/m/K and an effective volumetric heat capacity  $\rho c_p$  of  $2.47 \pm 0.29$  MJ/m<sup>3</sup>/K. The organic matter content in the peat sample (samples 7 in Figure 6) is 33%, twice the one measured in the organic clay samples (11-15%).

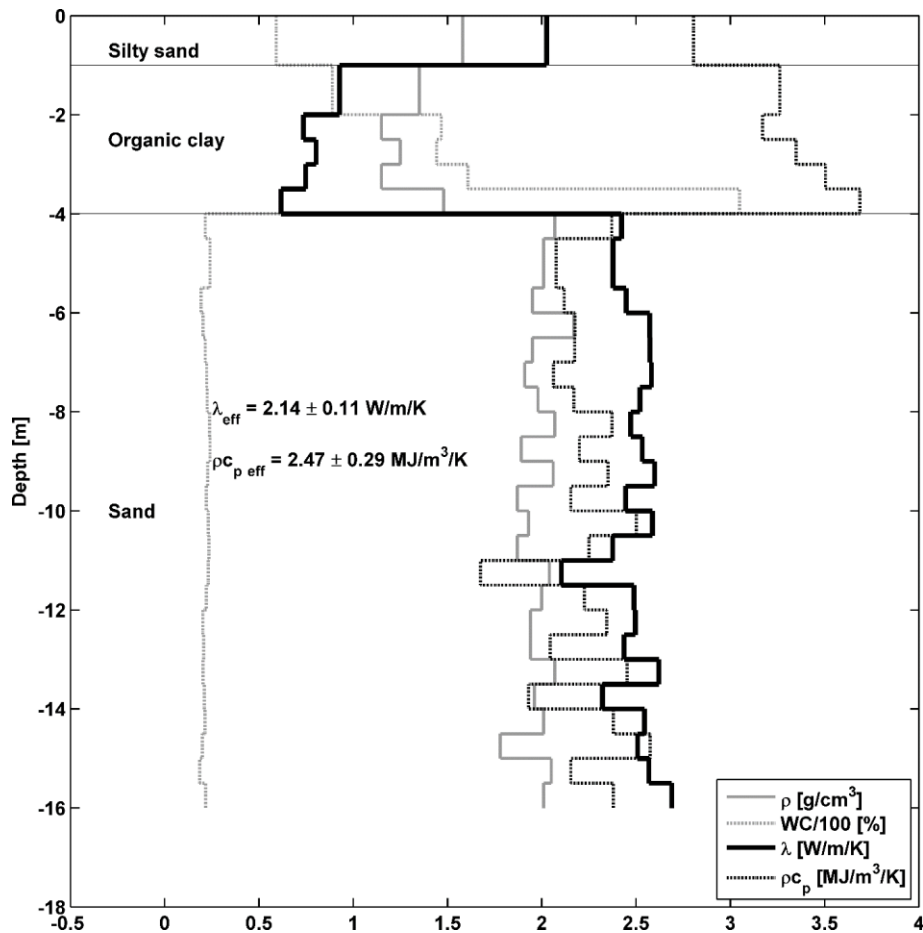


**Figure 7: Stratigraphic profile at Rosborg Norht test site. Bulk density  $\rho$ , water content, thermal conductivity  $\lambda_s$  and volumetric heat capacity  $\rho c_p$  measured in the laboratory using the Hot Disk apparatus are also provided.  $\rho c_{p, eff}$  and  $\lambda_{s, eff}$  are weighted average estimates over the length of the drilling.**



## 4. Thermal properties of concrete

This section aims to measure the thermal properties of the standard concrete (S3 receipt) produced at Centrum Pæle A/S. This receipt is used in the production of precast pile heat exchangers. First, the experimental characterisation of the concrete is provided. Then, the goodness of fit of thermal conductivity and heat capacity prediction models is assessed, by comparing their estimations to the measurements.

### 4.1. Experimental characterisation

First, the mix constituents and the test specimens are described, after, the laboratory work is summarised and the measurements shown. Later, selected prediction models are applied and to finish, both approaches are compared. The thermal expansion is not measured in this study.

#### 4.1.1. Mix constituents and test specimens

The studied mix is the one used in the production of precast pile heat exchangers (S3 receipt). Details of mix components, laboratory conditions for casting and compressive strength results are given in Table 1. A mineralogical analysis of the aggregates has been carried out (see Appendix B). Quartz is the main component (62%) for the pit sand, while crystalline rocks lead the gravel aggregates (61%). For the determination of the thermal properties, four sliced 100 x 200 mm cylinders were used: samples S1 and S2 belong to the same batch produced the 08/04/2016 while samples S3 and S4 belong to the batch produced the 19/01/2017. Every slide had a 65 mm thickness, approximately.

**Table 1: Mix components and physical properties for the S3 receipt. Average values for the two batches. The dosage is kept confidential.**

Components S3 receipt	
Cement (CEM I 52,5, Dyckerhoff Dreifach N)	-
Fly ash (Type B5)	-
Water	-
Air-entraining admixture (MicroAir)	-
Plasticizer (Glenium ACE 403)	-
Pit sand 0 - 2mm	-
Crushed stone 4 - 8 mm	-
Pea gravel 8 - 16 mm	-
Physical properties S3 receipt	
Water/cement ratio	0.40
Air content in fresh concrete [%]	3.25
Density [kg/m <sup>3</sup> ]	2370.00
Compressive strength at 28 days [Mpa]	66.2

#### 4.1.2. Measurements

For each specimen the following properties were measured in the laboratory: bulk dry density  $\rho_d$  [kg/m<sup>3</sup>], bulk saturated density  $\rho_s$  [kg/m<sup>3</sup>], bulk natural density  $\rho_n$  [kg/m<sup>3</sup>], water content or humidity [% of weight], porosity, absorption, thermal conductivity  $\lambda_c$  [W/m/K] and volumetric heat capacity  $\rho c_{pc}$  [MJ/m<sup>3</sup>/K].

The four specimens (S3 receipt) have been measured in oven dry, saturated and normally dry (ambient air) conditions. This way, the potential lower and upper limits and intermediate conditions for the thermal properties are covered. More information about these processes is provided in Appendix A. Table 2 provides the average porosity and absorption of the concrete specimens.

**Table 2: Measured porosity and absorption of the concrete specimens.**

Sample ID	Volume of permeable voids [%]	Absorption [%]
S1	9.4	4.1
S2	9.3	4.0
S3	8.5	3.6
S4	7.4	3.2
Average	8.6	3.7

Repeated measurements have been taken with the Hot Disk apparatus for each sample at a room temperature between 19 to 23°C for the three water content conditions (dry, saturated and normally dry), summarised in Table 3. More information about the measurements and the test are provided in Appendixes A and B.

**Table 3: Summary of samples and measurements for each condition.**

Sample ID	Condition	Number of measurements
S1	Oven dry	5
S1	Normally dry	15
S1	Saturated	10
S2	Oven dry	5
S2	Normally dry	15
S2	Saturated	10
S3	Oven dry	5
S3	Normally dry	5
S3	Saturated	10
S4	Oven dry	5
S4	Normally dry	5
S4	Saturated	10

The measured thermal properties of the four specimens are plotted in Figure 8. Each marker contains the average of five repeated measurements and the error bars comprise the 95% confidence interval, which account for systematic and random errors. The average values of the measurements in dry, normally dry and saturated conditions of the four specimens are summarised in Table 4 and illustrated in Figure 9. The measured values are in accordance with the values reported in Neville (1995).

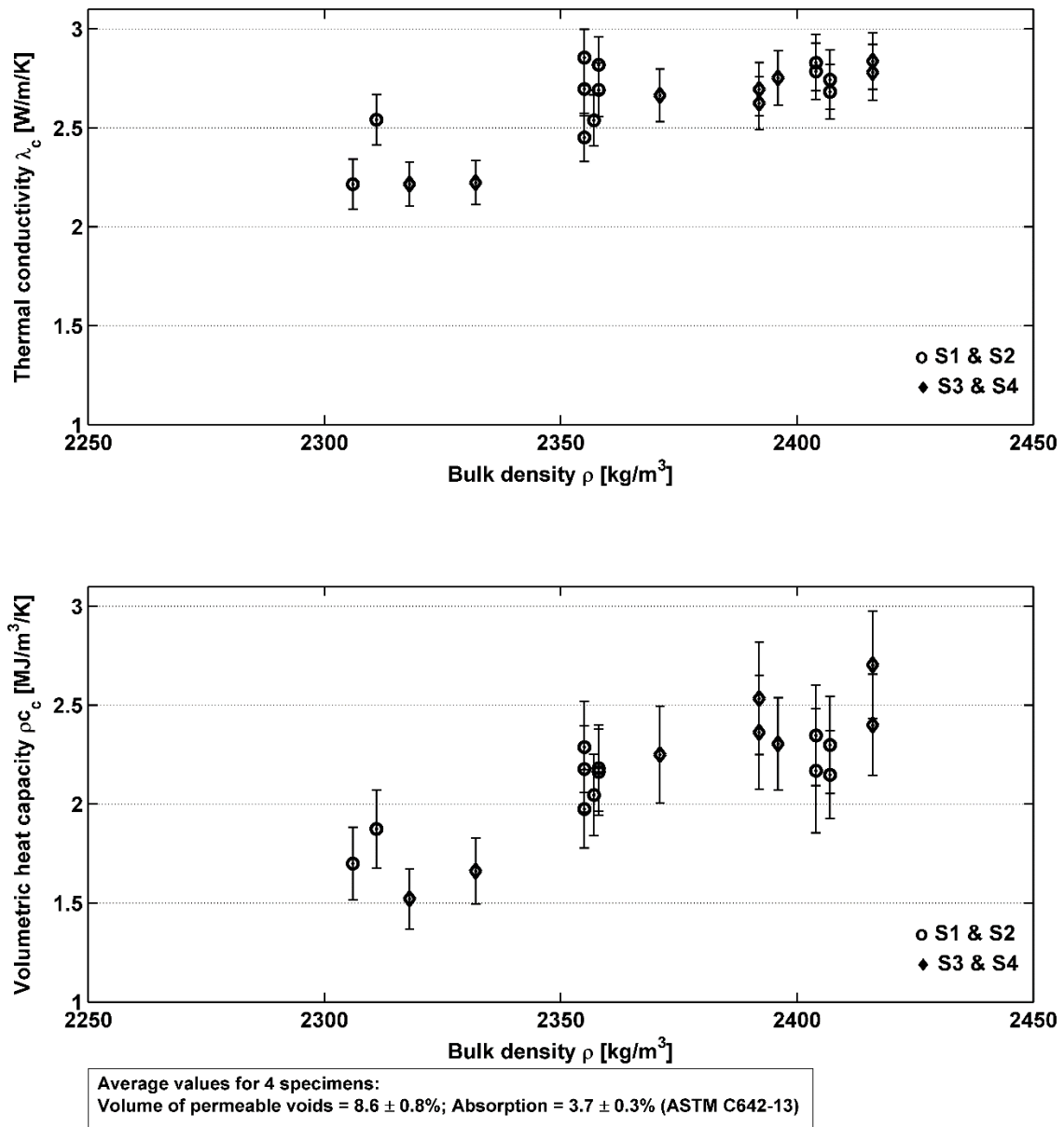


**Figure 8: Measured thermal properties of S3 receipt concrete with the transient plane source method. The error bars indicate the 95% confidence level.**

Due to a change in humidity of 3.7% (saturated conditions), the thermal conductivity of the dry concrete decreases up to 16% while the volumetric heat capacity decreases 28%. It is a considerable change, considering the low modification in humidity.

**Table 4: Summary of mean values of the thermal property property measurements and their uncertainties.**

Sample condition	Density $\rho$ [kg/m <sup>3</sup> ]	Thermal conductivity $\lambda_c$ [W/m/K]	Volumetric heat capacity $\rho c_{pc}$ [MJ/m <sup>3</sup> /K]
Oven dry	$2318 \pm 8$	$2.30 \pm 0.28$	$1.69 \pm 0.29$
Normally dry	$2370 \pm 16$	$2.69 \pm 0.18$	$2.17 \pm 0.24$
Saturated	$2405 \pm 9$	$2.75 \pm 0.15$	$2.37 \pm 0.28$

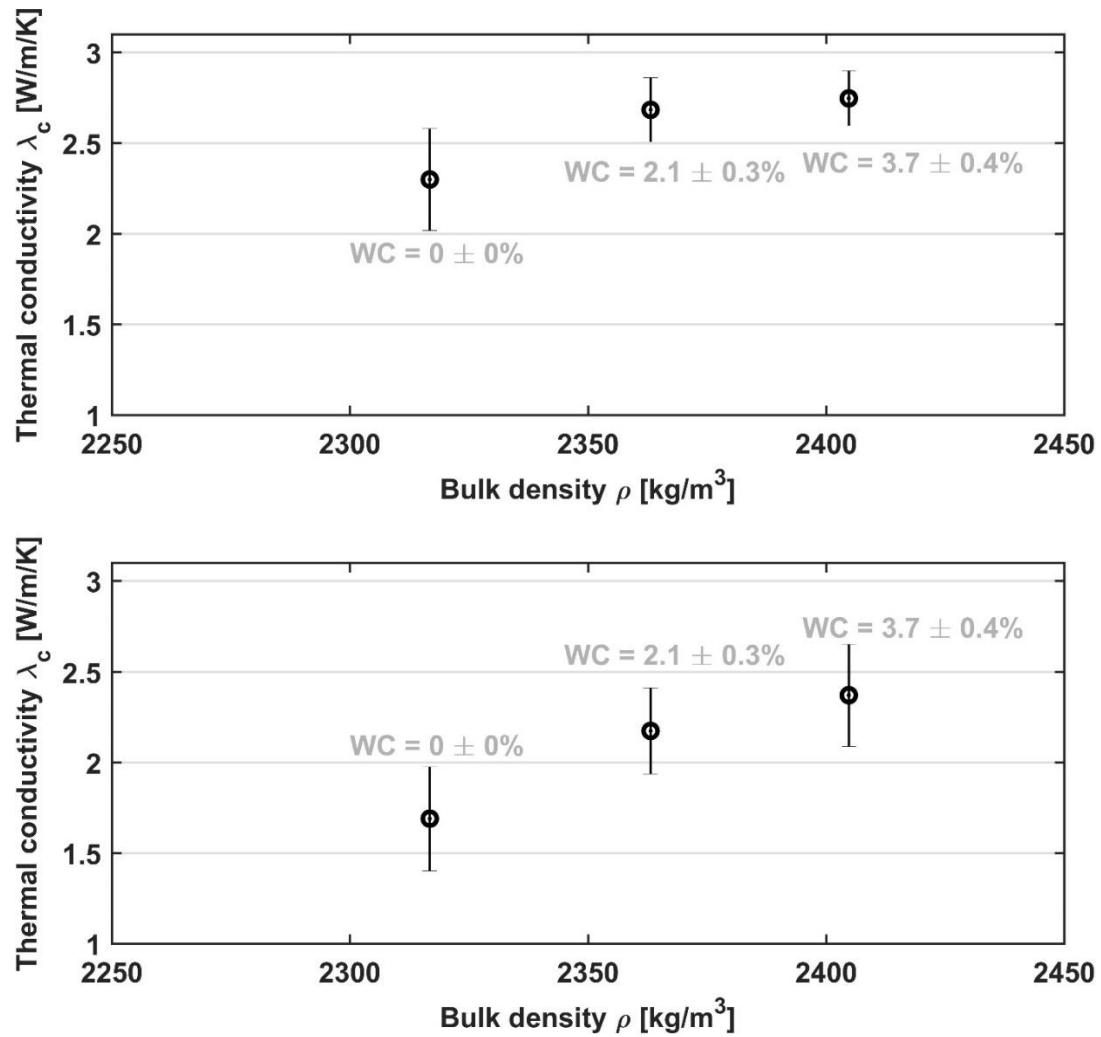


**Figure 9: Average of measured thermal properties of S3 receipt concrete with the transient plane source method. The error bars indicate the 95% confidence level. Average values for 4 specimens, according to ASTM C642-13: volume of permeable voids:  $8.6 \pm 0.8\%$ ; absorption =  $3.7 \pm 0.3\%$ .**

Pomianowski M. (personal communication, January 2017) suggests that the drying process of the concrete could take months and, therefore, the results reported in this study might not have been measured in completely dry conditions.

## 4.2. Application of prediction models of thermal properties

Campbell-Thorne's model (Equation 3) and the Hashin-Strikman's model (Equation 4) have been selected, as they have been considered more suitable since the pore nature (connections and shapes) is unknown in the studied concrete. For the volumetric heat capacity, the model of mixing theory is applied.

The use of prediction models requires to know the materials compounding the concrete. A mineralogical analysis of the aggregates has been done (Appendix C) and the main components have been identified for each aggregate. The continuous phase is defined as the cement paste and fly ash while the particle phase involved all the aggregates (the air content was neglected). The thermal properties considered for each of the components are given in Table 5. These values are chosen from the literature (Appendix B).

**Table 5: Thermal properties of the concrete components assumed for the prediction models.**

Components	Density $\rho$ [kg/m <sup>3</sup> ]	Mass fraction	Volume fraction	Thermal conductivity $\lambda$ [W/m/K]		Volumetric heat capacity $\rho c_p$ [MJ/m <sup>3</sup> /K]	
				Saturated state	Dry state	Saturated state	Dry state
Pit sand, 0/2 mm, main comp. quartz (62 %)	2640	0.27	0.25	6.00	5.00	2.10	2.00
Crushed stone, 4/8mm, main comp. crystalline (61 %)	2660	0.05	0.04	4.60	3.00	2.20	2.00
Pea gravel, 8/16mm, main comp. crystalline (61 %)	2650	0.45	0.40	4.60	3.00	2.20	2.00
Cement	3100	0.15	0.11	1.20	1.20	2.65	2.65
Fly ash (Bentz et al., 2011 & Kim et al., 2003)	2380	0.03	0.03	0.89	0.89	1.71	1.71
Water	1000	0.06	0.14	0.58	0.58	4.19	2.20
Air-entraining admixture (MicroAir)	-	-	-	-	-	-	-
Plasticizer (Glenium ACE 403)	-	-	-	-	-	-	-
Air (3%)	-	-	-	-	-	-	-

## 4.3. Discussion

As shown in Figure 10, the prediction models overestimate the measurements for dry conditions while they target very close the thermal properties in saturated conditions, as concluded by Khan (2002). Porous media approaches are recommended to get more information about the pore nature. The measured values are in accordance with the values reported in Neville (1995). However, the measurements seem very sensitive to the humidity content of the samples.

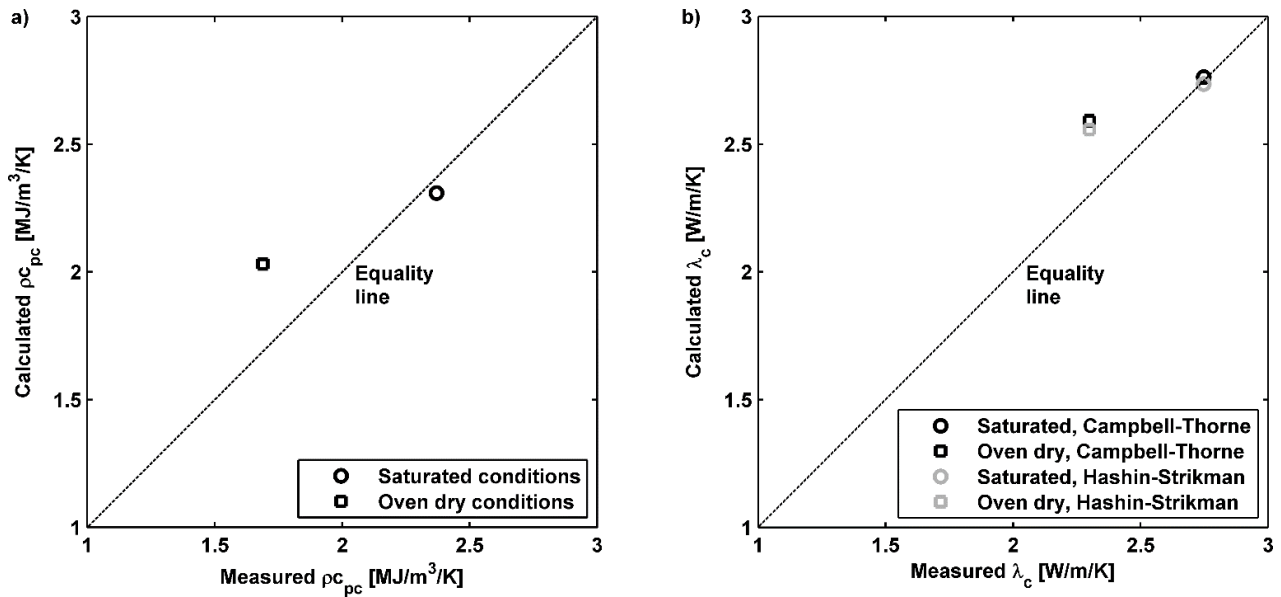


**Figure 10: Predicted thermal properties of concrete against experimentally obtained values a) volumetric heat capacity  $\rho_{pc}$  and b) thermal conductivity  $\lambda$ .**

## 5. Conclusion

Pile heat exchangers, also known as energy piles, are thermally active building foundation elements with embedded geothermal pipes fixed to the steel reinforcement in which a circulating fluid exchanges heat with the pile and the surrounding soil. As such, the foundation of the building both serves as a structural component and a heating/cooling supply element. The precast piles act as heat exchangers and, therefore, the thermal properties of the concrete and the surrounding soil highly influence the heat transfer phenomena within the pile-soil system.

This document measures the thermal properties of the soil from two locations and the standard concrete (S3 receipt) produced at Centrum Pæle A/S by means of the Hot Disk apparatus (transient plane source method), following Dansk Standard (2015).

The measurements of the soil specimens are in agreement with the ranges proposed in VDI (2010) and Abu-Hamdeh (2003). And the measurements for the concrete specimens are in accordance with the values reported in Neville (1995). However, the measurements seem very sensitive to the humidity content of the samples. A further comparison with prediction models of thermal properties has been done for the concrete samples. These models closely reproduce the thermal properties in saturated conditions but they differ in dry conditions, due to the complexity of considering the nature of pores.

Future research on the thermal properties of concrete should focus on: i) performing more measurements at different water contents and with different mixes to establish empirical rules to compute the thermal properties in terms of the bulk density. ii) Further study the nature of the pores of the concrete and analyse the validity of more complex prediction models, such as the ones recommended in Khan (2002). Regarding soil thermal properties, due to the fact that non-cohesive soils are harder to measure, unified measurement protocols should be developed, putting together the experience from several laboratories, so that the measured values are comparable.

## 6. Acknowledgements

We kindly thank the following financial partners: Centrum Pæle A/S, INSERO Horsens and Innovationsfonden Denmark. We express our deep gratitude to Victor Marcos Mesón for his advice and to Rosborg Gymnasium & HF and HKV Horsens for facilitating access to their installations.

## 7. References

- ABU-HAMDEH, N. H., 2003. Thermal Properties of Soils as affected by Density and Water Content. *Biosystems Engineering*, 86, 97-102.
- ALBERDI-PAGOLA, M., JENSEN, R. L. & POULSEN, S. E., 2016. A performance case study of energy pile foundation at Rosborg Gymnasium (Denmark). 12th REHVA World Congress Clima2016, 22-25 May 2016 Aalborg, Denmark. Department of Civil Engineering, Aalborg University, p. 10.
- ALBERDI-PAGOLA, M., POULSEN, S. E., JENSEN, R. L. & MADSEN, S., 2017. Thermal response testing of precast pile heat exchangers: fieldwork report. In: AALBORG UNIVERSITY, D. O. C. E. (ed.). Aalborg, Denmark: Aalborg University.
- ASTM STANDARDS, 1998. ASTM D2974:1998: Standard Test Methods for Moisture, Ash, and Organic Matter of Peat and Other Organic Soils. 1916 Race St., Philadelphia, PA 19103.
- ASTM STANDARDS, 2013. C642-13. Standard Test Method for Density, Absorption, and Voids in Hardened Concrete.
- BENTZ, D., PELTZ, M., DURAN-HERRERA, A., VALDEZ, P. & JUAREZ, C., 2011. Thermal properties of high-volume fly ash mortars and concretes. *Journal of Building Physics*, 34, 263-275.
- CHAN, J., 2014. Thermal properties of concrete with different Swedish aggregate materials. Rapport TVBM (5000-serie).
- DANSK GEOTEKNIK A/S, 1973. Geoteknisk rapport. Grundundersøgelser for Amtsgymnasium i Vejle, Vestre Engvej, Vejle.
- DANSK STANDARD, 2015. DS/EN ISO 22007-2 (2015): Plastics – Determination of the thermal conductivity and thermal diffusivity – Part 2: Transient plane heat source (hot disc) method.
- DEMIRBOĞA, R., TÜRKMEN, İ. & KARAKOÇ, M. B., 2007. Thermo-mechanical properties of concrete containing high-volume mineral admixtures. *Building and Environment*, 42, 349-354.
- DS/EN ISO/TS 17892-1: 2004 2004. Geotechnical investigation and testing - Laboratory testing of soil – Part 1: Determination of water content.
- DS/EN ISO/TS 17892-2: 2004 2004. Geotechnical investigation and testing - Laboratory testing of soil – Part 2: Determination of density of fine-grained soil.
- FRANCK GEOTEKNIK A/S, 2013. Geoteknisk rapport, parameterundersøgelse. Rosborg Gymnasium, Vestre Engvej 61, Vejle. Ny Nordfløj.
- GARBOCZI, E. J. & BENTZ, D. P., 1992. Computer simulation of the diffusivity of cement-based materials. *Journal of Materials Science*, 27, 2083-2092.
- HANSEN, K. K., 1986. Sorption isotherms: a catalogue. Technical University of Denmark Danmarks Tekniske Universitet, Department of Structural Engineering and MaterialsInstitut for Bærende Konstruktioner og Materialer.
- HOT DISK AB, 2014. Hot Disk Thermal Constants Analyser TPS 1500 unit, Intruction Manual.
- KHALIQ, W. & KODUR, V., 2011. Thermal and mechanical properties of fiber reinforced high performance self-consolidating concrete at elevated temperatures. *Cement and Concrete Research*, 41, 1112-1122.

- KHAN, M., 2002. Factors affecting the thermal properties of concrete and applicability of its prediction models. *Building and Environment*, 37, 607-614.
- KIM, K.-H., JEON, S.-E., KIM, J.-K. & YANG, S., 2003. An experimental study on thermal conductivity of concrete. *Cement and Concrete Research*, 33, 363-371.
- LARSEN, G., 1995. A guide to engineering geological soil description, dgf-bulletin, 1, revision 1 (May 1995). Danish Geotechnical Society, Lyngby.
- MARSHALL, A., 1972. The thermal properties of concrete. *Building Science*, 7, 167-174.
- MEHTA, P. & MONTEIRO, P. J. M., 2006. *Concrete: Microstructure, Properties, and Materials*, McGraw-Hill Education.
- NEVILLE, A. M., 1995. *Properties of concrete*.
- POMIANOWSKI, M., HEISELBERG, P., JENSEN, R. L., CHENG, R. & ZHANG, Y., 2014. A new experimental method to determine specific heat capacity of inhomogeneous concrete material with incorporated microencapsulated-PCM. *Cement and Concrete Research*, 55, 22-34.
- POMIANOWSKI, M.
- TAVMAN, I. H., 1996. Effective thermal conductivity of granular porous materials. *International Communications in Heat and Mass Transfer*, 23, 169-176.
- VDI, V. D. I., 2010. VDI 4640 Thermal Use of the Underground. Part 1: Fundamentals, approvals, environmental aspect. Berlin: VDI-Gesellschaft Energie und Umwelt (GEU).
- WADSÖ L., 2012. Thermal properties of concrete with various aggregates. *Cement and Concrete Research*.



## 8. Appendices

### A) Soils

This appendix provides pictures of the measurement process of soil thermal properties and information about the measurement parameters.

The cohesive samples were halved and in undisturbed conditions (Figures 11 and 12).



Figure 11: a) Halved moraine clay sample. b) Hot Disk kapton sensor ready to be placed between two specimens of soil. c) On-going Hot Disk testing, two-side measurement of a moraine clay sample (depth 8.5 m at Langmarsvej test site).

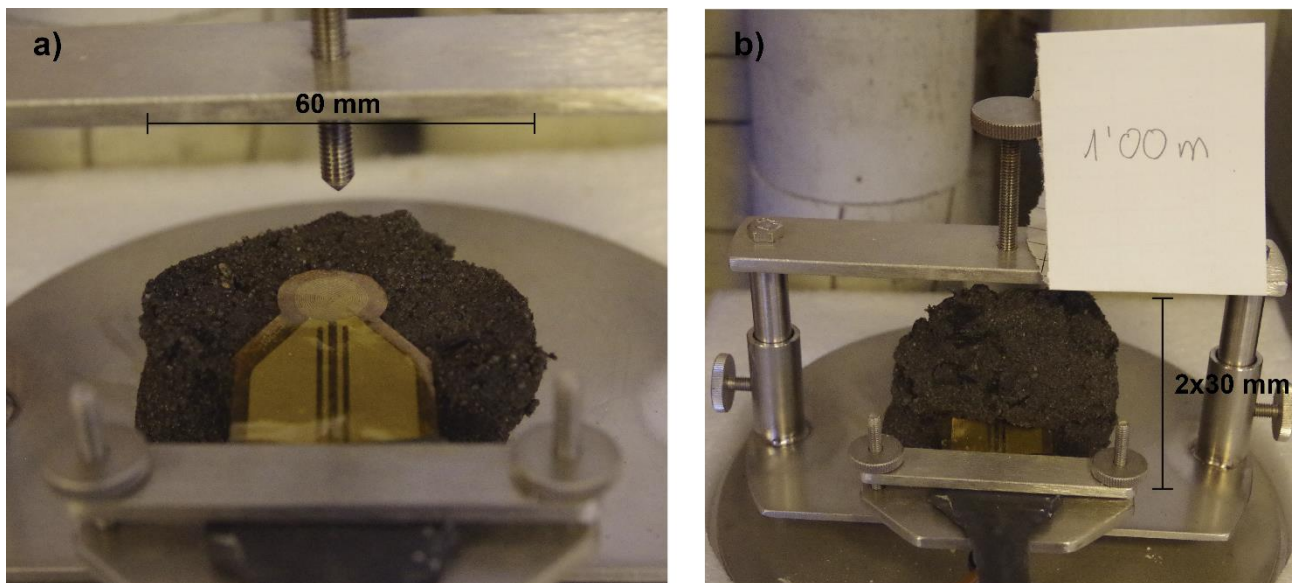
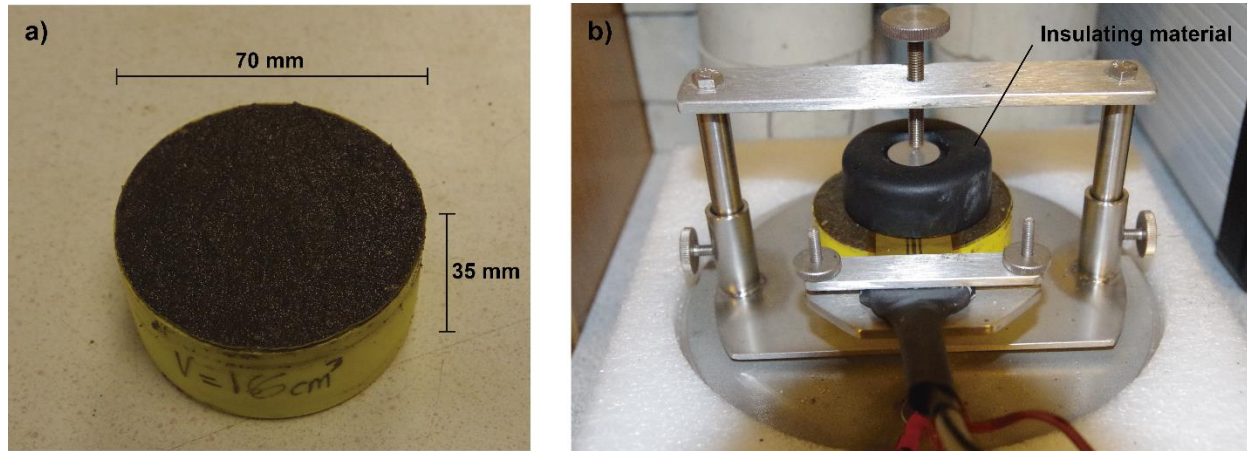


Figure 12: a) Hot Disk kapton sensor (15 mm in diameter) ready to be placed between two specimens of a silty sand sample. b) On-going Hot Disk testing, two-side measurement of the silty sand sample (depth 1.0 m at Rosborg North site).

Regarding non-cohesive samples, the sand was repacked into small containers to allow the single sided measurement procedure (Figure 13). The non-cohesive sample was taken off the sealed bag and placed into the containers layer by layer (1.5 cm approx.), compacting them with a hammer until the water (natural moist content) emerged to the surface.



**Figure 13: a) Sand sample in a container; b) On-going Hot Disk test, single-sided measurement of a sand sample (depth 4.5 m).**

Table 6 shows the parameters and sensors used for the measurement of different type of soils.

**Table 6: Summary of recommended experimental parameters for different soils based on measurements performed at the GeoLab at VIA University College, Horsens, DK, for the present study.**

Type of sample	Sand	Plastic clay	Clay till	Silty sand	Organic clay
Thermal conductivity [W/m/K]	2.40	1.30	2.30	2.03	0.80
Thermal diffusivity [mm <sup>2</sup> /s]	1.10	0.45	0.96	0.72	0.24
Temperature increase [K]	2.6	5.5	2.6	2.7	4.1
Sensor to use: Name/radius [mm]	8563 / 10	5501 / 6.5	5501 / 6.5	5501 / 6.5	5501 / 6.5
Specimen thickness [mm]	30	30	25	30	30
Specimen diameter [mm]	70	70	40	40	40
Measurement time [s]	80	80	40	40, 80	80
Heating Power [mW]	400, 800	250	400	250, 300	250

## B) Concrete

This appendix provides pictures of the measurement process of concrete thermal properties and gives information about the measurement parameters, the drying and saturating processes and the mineralogical analysis.

### Measurement process and parameters

The concrete samples were halved and measured as shown in Figure 14.

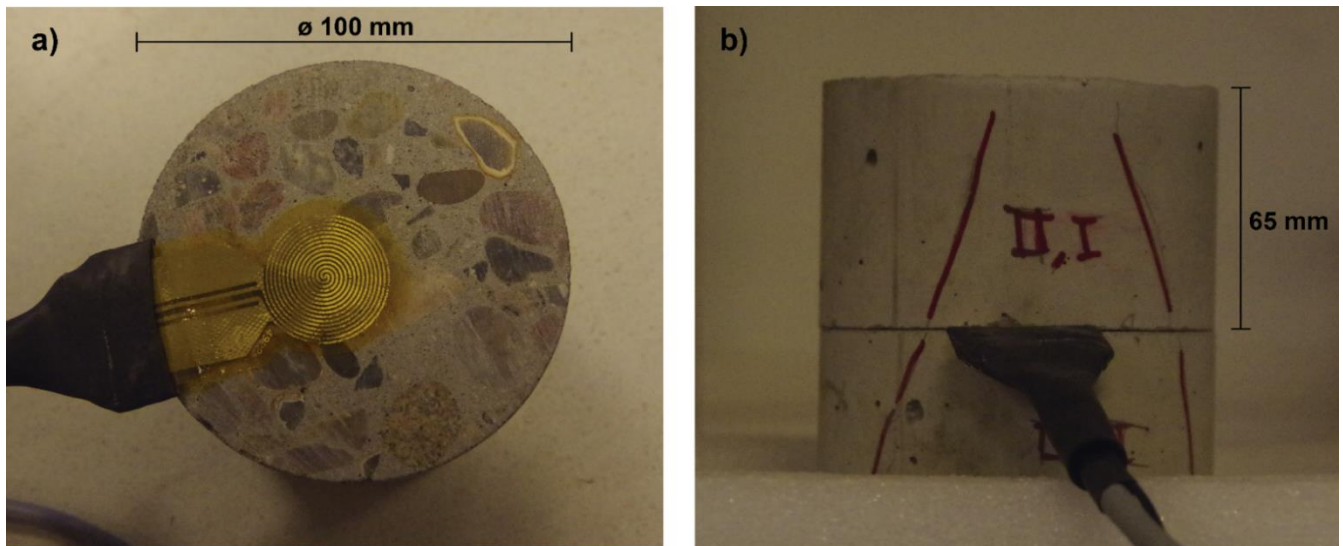


**Figure 14: a) Hot Disk kapton sensor (15 mm in diameter) ready to be placed between two specimens of concrete. b) On-going Hot Disk testing, two-side measurement of a concrete sample.**

Table 7 shows the parameters and sensors used for the measurement of concrete samples.

**Table 7: Summary of recommended experimental parameters for concrete specimens based on measurements performed at the GeoLab at VIA University College, Horsens, DK, for the present study.**

Type of sample	Concrete
Thermal conductivity [W/m/K]	2.11
Thermal diffusivity [mm <sup>2</sup> /s]	1.12
Temperature increase [K]	7.3
Sensor to use: Name/radius [mm]	4922/14.61
Specimen thickness [mm]	70
Specimen diameter [mm]	100
Measurement time [s]	80, 160
Heating Power [mW]	1000, 1200

## Oven drying and saturating concrete specimens

First, the drying in the oven was performed. After 48 hours of drying, the lost in humidity was below 0.2% from day 2 to 3 (Figure 15).

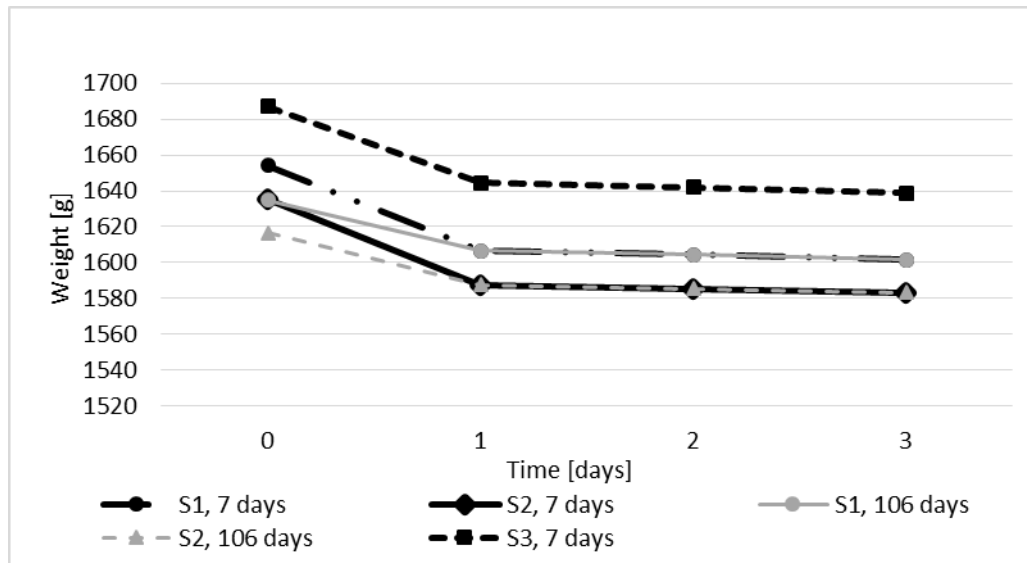


**Figure 15: Weight evolution over oven-drying process for each specimen. Concrete drying at 105 °C.**

Second, to measure the porosity and absorption of the concrete the following standard was followed ASTM C 642: 1975 (ASTM Standards, 2013). The specimens were vacuumed in a desiccator instead of boiled (Figure 16). Once saturated, the second round of measurements was made.



**Figure 16: Desiccator.**

## Measuring relative humidity in GeoLab and determining water content of normally dried specimens

The specimens, after saturation, were kept in the GeoLab at VIA University College for some days in order to normally dry them. The relative humidity and the temperature has been monitored over 2 days (Figure 17). The average temperature is 21 °C while the relative humidity is 40.5 %. According to Hansen (1986) in pp- 41, a concrete with a water-cement ratio of 40 at 20 °C the hygroscopic content at a relative humidity of 40 % is around 1.2 weight %. In this study it has been measured as 2.1%.



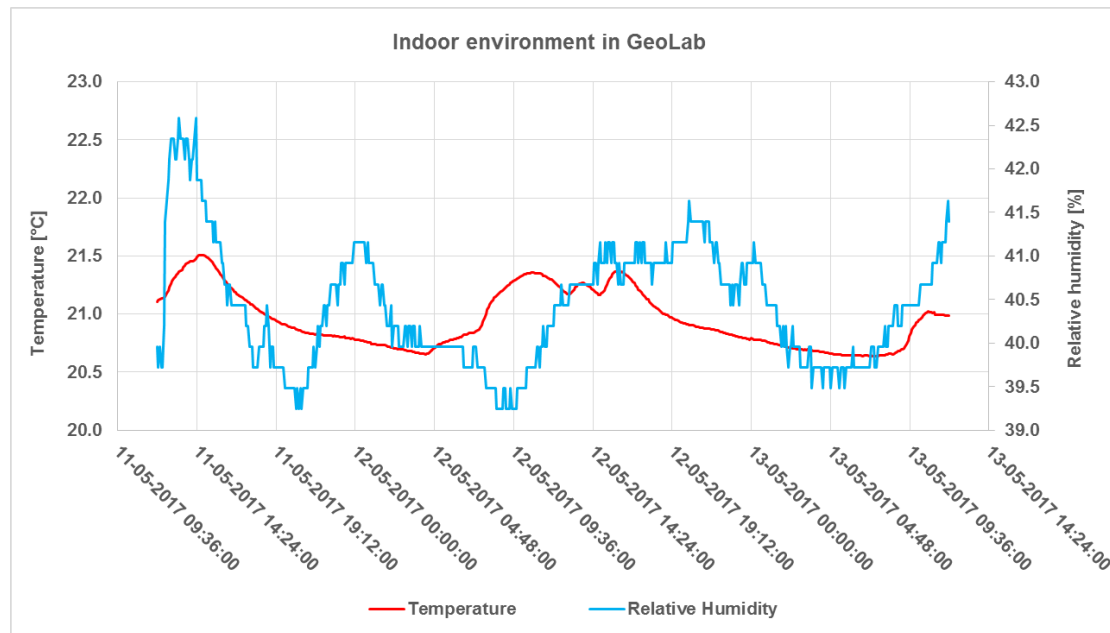


**Figure 17: temperature and relative humidity measurements in the GeoLab at VIA University College in Horsens (DK).**

## Mineralogical analysis

The three types of aggregate have been analysed, prior cleaning and drying. For the Sand 0 – 2 mm, the fraction bigger than 1 mm has been analysed. Table 8 shows the composition of the sample. The main component in the pit sand is quartz.

**Table 8: Mineralogical analysis of sand 0-2 mm.**

Type	Number of grains	Composition [%]
Quartz	247	62
Crystalline	79	20
Flint	34	9
Sedimentary	14	4
Unstable	24	6
Total	398	100

For the Gravel 4 – 8 mm, Table 9 shows the composition of the sample. The main components in the crushed stone are crystalline rocks, such as granite.

**Table 9: Mineralogical analysis of sand 4-8 mm.**

Type	Number of grains	Composition [%]
Quartz	2	2
Crystalline	60	61
Flint	26	26
Sedimentary	11	11
Unstable	0	0
Total	99	100

For the gravel 8-16 mm the same mineralogy as for gravel 4-8 mm has been assumed.

## Thermal property values from literature

The reference values for the thermal properties have been obtained from VDI (2010) and they are summarised in Table 10. These values are used for the prediction models.

**Table 10: Thermal property values considered for prediction models.**

Type of rock	Thermal conductivity [W/m/K]	Volumetric heat capacity [MJ/m <sup>3</sup> /K]	Density [kg/m <sup>3</sup> ]	Reference
Quartzite	5.0 - 6.0	2.1	2500 - 2700	VDI 4640 (2010)
Crystalline	1.9 - 4.6	1.8 - 2.6	2500 - 2700	
Flint	4.5 - 5.0	2.2	2500 - 2700	
Sedimentary	2.1 - 4.1	2.1 - 3.0	2200 - 2700	
Unstable rock	-	-	-	-

